ATLANTIS PRESS
Advances in Computer Science Research, volume 74
2nd International Conference on Computer Engineering, Information Science & Application Technology (ICCIA 2017)

Improved FastSLAM based on EnKF proposal distribution for AUV

Jing Wang [a,*], Zhenye Liu [b]
Tianjin JinHang Institute of Computational Technology, Tianjin, China
[a]wangjing8357@163.com, [b]liuzhenye8357@163.com

Keywords: AUV; FastSLAM; Particle degeneration; EnKF; Rao-blackwellised Particle filter (RBPF).

Abstract. A new Fast simultaneous localization and mapping (FastSLAM) algorithm based on ensemble Kalman filter (EnKF) is proposed in order to solve the problem of particles degeneration, which is an avoidless drawback in standard FastSLAM. This will decrease the estimated accuracy of autonomous underwater vehicle (AUV) location. Integrating the latest observe information, EnKF is used to produce the proposal distribution.， and it more approximates the real posterior distribution. The kinematic model of AUV, feature model and measurement models of sensors were established. Two experiments with improved FastSLAM were carried out to validate the effectiveness. The first experiment was complete simulation which showed that the presented method was feasible theoretically. The second experiment was based on trial data which showed that the method weakened the degradation and enhanced the accuracy and stability of AUV navigation and localization in practical application.

1. Introduction

The development of AUV has brought numerous advantages, and also presented more challenges. The problem of underwater navigation is one of the most significant examples. Traditionally, the problem could be addressed in several ways, none of which being fully adequate. The positional error grows with dead reckoning[1] based on Inertial Navigation Systems (INS) or Doppler Velocity Logs (DVL), which make them impractical for long time navigation. In order to avoid this problem, Global Positioning System (GPS) can be used to provide navigation resets, but due to the null in underwater environments, it can only be effective when on the surface. What's more, artificial beacons could be employed for long term underwater positioning. Many configurations are available for these beacon systems, such as Long Base Line (LBL), Short Base Line (SBL) or Ultra Short Base Line (USBL). Unfortunately, there are numerous missions, in which these solutions are not suitable. So, a self-contained system would be better, without previous information of the environment or any external devices to obtain a reliable localization of the AUV.

In unknown or partly known environment, with self location and pose uncertain, AUV makes use of onboard sensors to apperceive surroundings and perform localization and mapping simultaneously, which is called SLAM. This ability is considered as a prior condition of AUV autonomy. Recently, various methods are presented to solve the SLAM problem indoor, outdoor, in the air and underwater. The limit of sensing ability of underwater sensors makes underwater SLAM become a great challenge.

Basic process of underwater SLAM is described as follows：The location estimated error of moving AUV will be accumulated during dead reckoning as a consequence of system noise and measurement noise or the inaccuracy of the prediction model (Figure 1a). However, An AUV navigation and localization system which performs SLAM is able to attenuate this uncertainty growth by means of repetitive observation of landmarks in the map. Figure 1b represents the situation where a new observation from AUV corresponds to an entity already incorporated in the map. Then a data association process should be adopted to determine whether the measurement is a visited landmark or a new one. If the landmark was visited, this information is used to update position of both of the AUV and map features. If not, the landmark will be added to the map. Adding more information makes a better estimate and a reduction of error in the problem (Figure 1c).

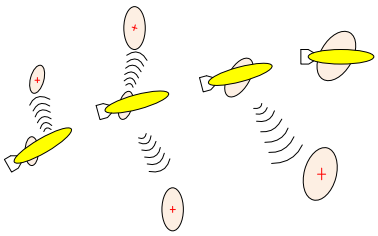

Fig.1a Growth of landmarks and AUV uncertainty

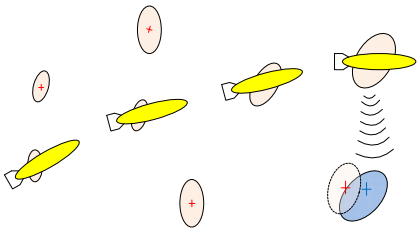

Fig.1b New measurement (blue) is a re-observation of landmark in the map

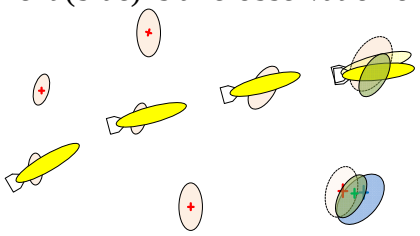

Fig.1c Incorporating new information results in a better estimate (green) of both map and AUV

SLAM is becoming a more and more popular topic in underwater robotic field. Tena from Heriot-Watt University realized SLAM with stochastic map based on augment EKF [2-5]. Eustice from Woods Hole Oceanographic Institution performed SLAM with Augmented State Kalman filter using a camera in an unstructured environment. Roman from MIT and Singh from Woods Hole Oceanographic Institution proposed a method to improve bathymetric mapping using SLAM. The solution consisted of generating a set of sub-maps from small bathymetric patches created over short periods of time[6]. West from University of Hawaii presented a robust extended Kalman filter (REKF)[7]. David from Girona University summarized the previous SLAM methods and realized SLAM with EKF and local map joining approach [8]. Barkby from University of Sydney demonstrated that the uncertainty in the vehicle state can be modeled using a particle filter and an extended Kalman filter (EKF), where each particle maintains a 2D depth map to model the seafloor[9]. In summary, EKF-SLAM is a common SLAM frame; however, it suffers the influence of system model linearization, computational complexity and amphibolous data association. UKF-SLAM is an extended version of EKF-SLAM. It is suitable for nonlinear motion of AUV [10,11]. EIF-SLAM is good at a low computational cost when compared with EKF-SLAM [12, 13]. FastSLAM based on Rao-blackwellised particle filter (RBPF) is another prevail frame [14], it is unlimited to the nonlinear and non-gauss system. It is more advanced than EKF-SLAM in both the nonlinear model and computational complexity, but the standard FastSLAM takes the prior distribution as the proposal distribution, its biggest drawback is the degradation of particles in resampling progress.

An improved FastSLAM method based on EnKF proposal distribution is proposed in order to solve this degradation phenomenon. An effective method to enhance the capability of PF is an appropriate proposal distribution. EnKF is used to generate the proposal distribution every step. It more approximates the true posterior probability density, and the computation load is less. Eventually， one experiment based on complete simulation and the other based on trial data were carried out to validate the efficiency of the method.

2. Improved FastSLAM based on EnKF Proposal

2.1 The Generation of EnKF Proposal

The essence of EnKF is a Kalman filter based on Monte Carlo. High computational efficiency and the capacity of processing non-gauss and nonlinear system make EnKF used widely in the field of weather forecast [15]. The main idea is initializing a set of system state as the background set, and analyzed set is obtained through updating the individual of background set with Kalman filter. The true mean and covariance of the state are estimated with analyzed set. Passing the set of sample by system model, the background set of next moment is obtained.

The set $X_k^b = \{x_{k,i}^b, i = 1,2,\ldots n\}$ is the background state set at time k, which is transferred by the analyzed set at time $k-1$. n is the number of samples. The mean and variance could be computed by the following expressions:

$$\hat{x}_k^b = \frac{1}{n}\sum_{i=1}^{n} x_{k,i}^b \tag{1}$$

$$\hat{P}_k^b = \frac{1}{n-1}\sum_{i=1}^{n}\left(x_{k,i}^b - \hat{x}_k^b\right)\left(x_{k,i}^b - \hat{x}_k^b\right)^{\mathrm{T}} \tag{2}$$

In the practical application, $\hat{P}_k^b$ can be instead by the following expression:

$$\hat{P}_{xh}^k = \frac{1}{n-1}\sum_{i=1}^{n}\left(x_{k,i}^b - \hat{x}_k^b\right)\left(h\left(x_{k,i}^b\right) - h\left(\hat{x}_k^b\right)\right)^{\mathrm{T}} \tag{3}$$

$$\hat{P}_{hh}^k = \frac{1}{n-1}\sum_{i=1}^{n}\left(h\left(x_{k,i}^b\right) - h\left(\hat{x}_k^b\right)\right)\left(h\left(x_{k,i}^b\right) - h\left(\hat{x}_k^b\right)\right)^{\mathrm{T}} \tag{4}$$

The ensemble Kalman gain is:

$$K_k = \hat{P}_{xh}^k\left(\hat{P}_{hh}^k + R_k\right)^{-1} \tag{5}$$

R_k is the observation error covariance matrix at time k.

With the latest observation information, the background set is updated, and the analyzed set $X_k^a = \{x_{k,i}^a, i = 1,2,\ldots n\}$ is obtained,

$$x_{k,i}^a = x_{k,i}^b + K_k\left(y_{k,i} - h\left(x_{k,i}^b\right)\right), i = 1,2,\ldots,n \tag{6}$$

Accordingly, the mean and the covariance of the analyzed set is :

$$\hat{x}_k^a = \frac{1}{n}\sum_{i=1}^{n} x_{k,i}^a \tag{7}$$

$$\hat{P}_k^a = \frac{1}{n-1}\sum_{i=1}^{n}\left(x_{k,i}^a - \hat{x}_k^a\right)\left(x_{k,i}^a - \hat{x}_k^a\right)^{\mathrm{T}} \tag{8}$$

EnKF is used to estimate the posterior probability density recursively. In the frame of FastSLAM, a special EnKF is used by every particle. EnKF and the latest observation information are used to update the mean and covariance of every particle at time $k-1$, and new particles are sampled from the distribution.

Different from EKF, EnKF does not need to linearize the nonlinear equation and the computation of Jacobian matrix is avoided. The estimate accuracy is enhanced and the computation is reduced by using the set to estimate the statistic value. Especially for the non-differentiable and nonlinear system, the advantage is more obviously.

2.2 FastSLAM based on EnKF Proposal Distribution

The posterior of FastSLAM decomposes into a product of $K+1$ recursive estimators: one estimator over AUV paths, and K independent estimators over landmark positions, each conditioned on the path estimate. So the SLAM posterior could be represented as:

$$p\left(s^t, \Theta \middle| z^t, u^t, n^t\right) = \underbrace{p\left(s^t \middle| z^t, u^t, n^t\right)}_{path\ posterior}\underbrace{\prod_{k=1}^{K} p\left(\theta_k \middle| s^t, z^t, u^t, n^t\right)}_{landmark\ estimate} \tag{9}$$

where superscript t represents the set of all the variables from 1 to t. $s^t = s_1, s_2, \cdots s_t$ is the path estimate of AUV; $z^t = z_1, \cdots z_t$ is the observation of each landmark; $u^t = u_1, \cdots u_t$ is the control vector;

$\Theta = \{\theta_1, \cdots \theta_K\}$ is the set of all the landmark; $n^t \in \{1, \cdots K\}$ is the index of landmark which is perceived at time t.

Particle filter based on EnKF (EnKPF)is used to estimate the path of AUV. Extended Kalman filter is used to estimate the location of landmarks. Since the estimate of landmarks depends on the estimate of the AUV path and each particle is a trajectory of AUV with all the landmarks as shown in figure 2. Therefore, if there are M particles and every particle contains K landmarks, there will be MK extended Kalman filters in total.

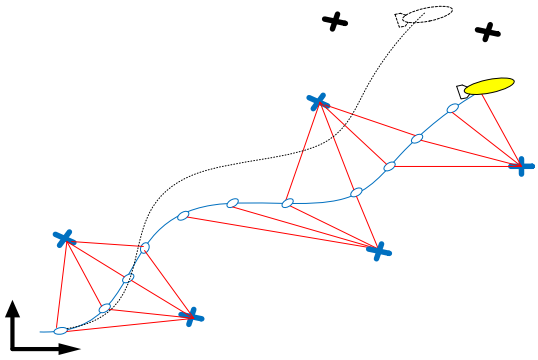

Fig.2 Illustration of a particle

2.2.1 Estimate of AUV Path

EnKF is used to estimate the posterior distribution of AUV path $p\left(s^t \middle| z^t, u^t, n^t\right)$ in improved FastSLAM. The steps of the algorithm are as follows:

Step1 Initialize and obtain the initial particle set.

Step2 Define the background set and predict the background set at time k. Compute the mean and covariance of the background set.

Step3 Compute the ensemble Kalman gain.

Step4 Update the particles with the EnKF and obtain the analyzed set. Then the mean and covariance could be got.

Step5 Proposal distribution function is established with the analyzed set. New particles are sampled and the weight of every particle is computed.

Step6 Normalize the weights.

Step7 Resample.

Step8 Output the state at time k.

A set of particles are used to represent this posterior, and will be written as S_t. Each $s^{t,[m]} \in S_t$ denotes an estimate of AUV paths:

$$S_t = \left\{s^{t,[m]}\right\} = \left\{s_1^{[m]}, s_2^{[m]}, \cdots, s_t^{[m]}\right\} \tag{10}$$

the superscript $^{[m]}$ represents the m-th particle in set.

Particle set S_t is calculated incrementally from particle set S_{t-1} at time $t-1$, control vector u_t and observation vector z_t. Draw samples from the proposal distribution, and correct for the difference using a technique called importance sampling.

The proposal distribution based on EnKF generates guesses of the AUV's pose at time t given each particle $s^{t-1,[m]}$.This guess is obtained by sampling from the motion model.

$$s_t^{[m]} \sim p\left(s_t \middle| u_t, s_{t-1}^{[m]}\right) \tag{11}$$

This estimate $s_t^{[m]}$ is added to a temporary set of particles, along with the path S_{t-1}. We can get new particles drawn from the proposal distribution, and they are distributed according to:

$$p\left(s^t \middle| z^{t-1}, u^t, n^{t-1}\right) \tag{12}$$

2.2.2 Estimate of Landmark Location based on EKF

EKF is used to estimate the location of landmarks in improved FastSLAM. Since the landmark estimates are conditioned on the AUV's path, EKFs are attached to each particle in S_t. So the posterior of the entire path and landmarks is represented with particle set as follows:

$$Particle_t = \left\{ s^{t,[m]}, \mu_1^{[m]}, \Sigma_1^{[m]}, \cdots, \mu_k^{[m]}, \Sigma_k^{[m]} \right\} \tag{13}$$

where $\mu_k^{[m]}, \Sigma_k^{[m]}$ is the mean and covariance of the m-th particle and the k-th landmark respectively.

The posterior over the k-th landmark position is easily obtained. Its computation depends on whether $n_t = k$. If $n_t = k$, the landmark θ_k was observed at time t. We can get

$$\begin{aligned} & p\left(\theta_k \middle| s^t, z^t, u^t, n^t\right) \\ & \overset{\text{Bayes}}{\propto} p\left(z_t \middle| \theta_k, s^t, z^{t-1}, u^t, n^t\right) p\left(\theta_k \middle| s^t, z^{t-1}, u^t, n^t\right) \\ & \overset{\text{Markov}}{=} p\left(z_t \middle| \theta_k, s_t, n_t\right) p\left(\theta_k \middle| s^{t-1}, z^{t-1}, u^{t-1}, n^{t-1}\right) \end{aligned} \tag{14}$$

If $n_t \neq k$, the landmark θ_k was observed first time, then

$$p\left(\theta_k \middle| s^t, z^t, u^t, n^t\right) = p\left(\theta_k \middle| s^{t-1}, z^{t-1}, u^{t-1}, n^{t-1}\right) \tag{15}$$

This process is data association. $n_t = k$ means that the new measurement corresponds to the feature that was already in the map, and EKF is used to update the location of landmark. $n_t \neq k$ means that this measurement doesn't corresponds to any feature in the map, and the augmentation of map will be performed.

3. System Model for AUV SLAM

3.1 Kinematic Model of AUV

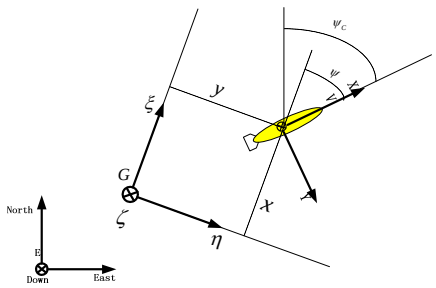

Fig.3 Global coordinate G and vehicle coordinate V

A global frame G and a vehicle frame V should be estimated first. The starting location of AUV is chosed as the origin of the global coordinate. See figure 3, ψ_C is the angle between the initial AUV heading and magnetic north in the earth global frame. A simple 4 DOF constant velocity kinematics model is used to predict how the state will evolve from time 1 to time t

$$\boldsymbol{X}_V(k) = f(\boldsymbol{X}_V(k-1), \boldsymbol{n}(k-1)) \tag{16}$$

Obviously, this model is nonlinear. And its detail form is (11). $[x, y, z, \psi]$ represents the position and heading of the AUV in the global frame G while $[u, v, w, r]$ are their corresponding linear and angular velocities on the vehicle's coordinate frame V. $\boldsymbol{n} = [n_u, n_v, n_w, n_r]$ represents an acceleration white noise additive in the velocity terms. Since the model doesn't account for the roll and pitch, it is approximate, and cannot match with actual model absolutely.

$$\begin{bmatrix} x \\ y \\ z \\ \psi \\ u \\ v \\ w \\ r \end{bmatrix}_{(k)} = \begin{bmatrix} x+\left(u\mathrm{T}+n_u\frac{\mathrm{T}^2}{2}\right)\cos\psi-\left(vT+n_v\frac{\mathrm{T}^2}{2}\right)\sin\psi \\ y+\left(u\mathrm{T}+n_u\frac{\mathrm{T}^2}{2}\right)\sin\psi+\left(v\mathrm{T}+n_v\frac{\mathrm{T}^2}{2}\right)\cos\psi \\ z+w\mathrm{T}+n_w\frac{\mathrm{T}^2}{2} \\ \psi+r\mathrm{T}+n_r\frac{\mathrm{T}^2}{2} \\ u+n_u\mathrm{T} \\ v+n_v\mathrm{T} \\ w+n_w\mathrm{T} \\ r+n_r\mathrm{T} \end{bmatrix}_{(k-1)} \tag{17}$$

3.2 Measurement Model

AUV is deployed with compass, DVL and pressure sensor to supply heading, velocity and depth in state vector, so the measurement model is linear. Their common model is written as:

$$\boldsymbol{z}(k)=\boldsymbol{HX}(k\mid k-1)+\boldsymbol{m}(k) \tag{18}$$

where $\boldsymbol{z}$ is observation vector, $\boldsymbol{H}$ changes according to different measurement. $\boldsymbol{m}$ is the noise which affects the measurement process.

Mechanically scanning image sonar is used to apperceive the surroundings whose return is represented in the sonar coordinate when the line was detected. Data association process will be performed in order to determine whether the measurement is new or visited. First the feature in the map should be transformed to the vehicle coordinate currently:

$$\boldsymbol{z}_i^{\mathrm{V}}=\begin{bmatrix}\rho_i^{\mathrm{V}} & \theta_i^{\mathrm{V}}\end{bmatrix}^{\mathrm{T}}=h(\boldsymbol{X}(k),\boldsymbol{s}_i) \tag{19}$$

where ρ_i^{V} and θ_i^{V} are the representations of line in vehicle frame, ρ_i and θ_i are the representation in global frame. $\boldsymbol{s}_i$ is the observation noise.

4. Experiments

Two experiments are performed in order to validate the availability of the presented method.

Experiment 1: It was an absolute simulation in an area of 250m*200m. The velocity of AUV was set to 3m/s. The maximum steering angle was set to $\pi/6$. The sensor was set to a range of 30 m. The particle number was set to $M=100$.The sample number of EnKF was set to 50.

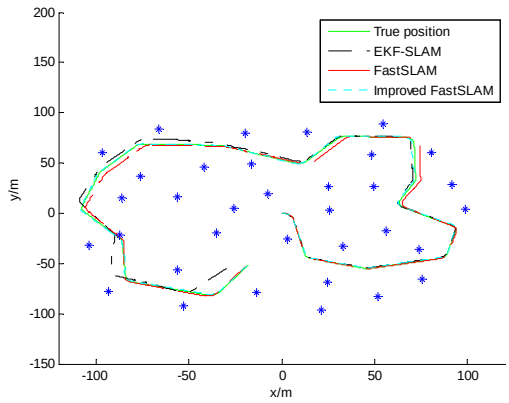

Fig.4 Estimated location comparison of three method

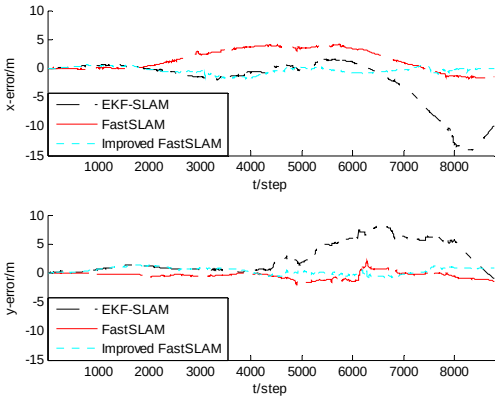

Fig.5 Error comparison of three method

In figure 4, the estimated positions of EKF-SLAM, FastSLAM and improved FastSLAM are displayed. The marker "*" stands for the location of true landmark. The accuracy of EKF-SLAM is not well because of the linearization of the nonlinear system model and non-gauss noise. The standard FastSLAM with prior probability density as the proposal distribution is better without the influence of linearization and non-gauss noise. Obviously, the improved FastSLAM is the best, because the EnKF was selected as the proposal distribution, which has more overlap area with posterior probability density than selecting prior probability density in standard FastSLAM. In figure 5, the estimated error of improved FastSLAM is less than both the standard FastSLAM and the EKF-SLAM. Apparently, the presented improve FastSLAM method is feasible in theory.

Experiment 2: In order to validate the feasibility in practice. The second experiment with trial data which was obtained by the researchers of Girona University was carried out. The velocity of AUV moved at about 0.2m/s. The data was composed of the measurement from DVL, Compass, mechanically scanning image sonar which was set to a range of 50 m, with a resolution of 0.1m and 1.8°. The moving trend of AUV is described as the curve in Figure 5, and the moving time of AUV was about 20min. The particle number is set to $M = 100$. The sample number of EnKF is set to 50.

Fig.6 Satellite photo of experimental environment

The comparison of EKF-SLAM， standard FastSLAM and improved FastSLAM in the estimate of AUV trajectory is shown in Figure 7. The result of EKF-SLAM is worst because it only uses the first order Taylor expansion of dynamic model of actual AUV. The standard FastSLAM is a little better because it does not linearize the dynamic model. The improved FastSLAM based on EnKF is the best. With the EnKF as the proposal distribution, the latest observation was added before computing the weights of particles. The proposal distribution more approximated the real distribution. After resampling, most particles were reserved. So the degradation of particles was reduced and the particle diversity was kept. The impoverished degree of particles was decreased.

Figure 8 is the north error curve and east error curve respectively with improved FastSLAM, standard FastSLAM and EKF-SLAM. Apparently, the accuracy is enhanced greatly with improved FastSLAM.

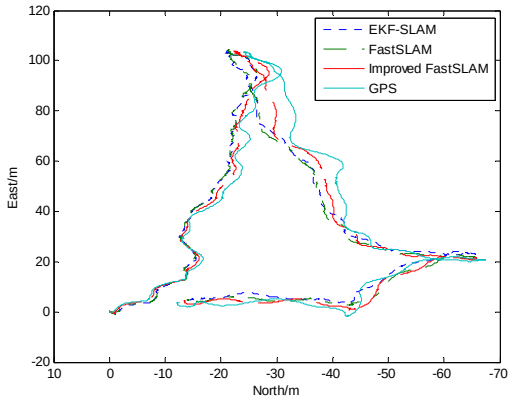

Fig.7 Comparison of navigation results of variance reduction FastSLAM, FastSLAM, EKF-SLAM and GPS

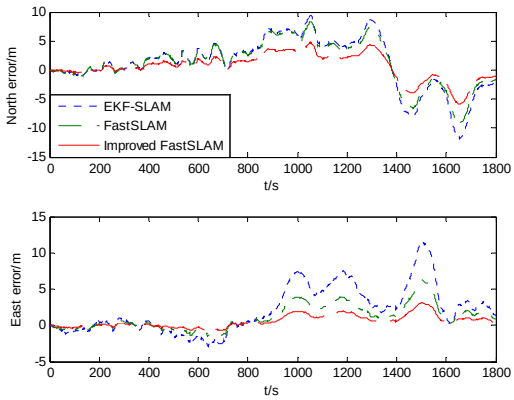

Fig.8 Error curves of north and east direction

5. Conclusion

Two experiments show that improved FastSLAM with EnKF as the proposal distribution has higher accuracy. It makes use of the advantage of EnKF. The particle degradation was reduced, and the particle diversity was kept in a certain extent. Especially the designed method is robust for the degradation caused by the model established not match with the actual kinematic model. The accuracy and stability of AUV SLAM system were improved obviously via the improved FastSLAM. It is significant for the AUV to execute long term sea environment monitor and other underwater work. The presented method is proved available in middling structured environment, and the SLAM in large unstructured environment is the key point in the future.

References

[1]. H. C. Brown, R. M Eustice, An Overview Autonomous Underwater Vehicle Research and Testbed at PeRL, MARINE TECHNOLOGY SOCIETY JOURNAL, 43(2) (2009), 33-47

[2]. I. Tena, Enhanced Concurrent Mapping and Localisation Using Forward-looking Sonar. PhD thesis. Heriot-Watt University. 2001: 35-48

[3]. E. Olson, J.J. Leonard, S.Teller, Robust range-only beacon localization, IEEE JOURNAL OF OCEANIC ENGINEERING, 31(4)(2006), 949-958

[4]. D. Ribas, P. Ridao, J.D. Tardos, Underwater SLAM in Man-Made Structured Environments, JOURNAL OF FIELD ROBOTICS, 25(11-12)(2008),898-921

[5]. A. Mallios, P. Ridao, M. Carreras, Navigating and Mapping with the SPARUS AUV in a Natural and Unstructured Underwater Environment, in: Proc. Oceans, 2011, 1-7

[6]. M.F. Fallon, G. Papadopoulos, J.J. Leonard and N.M. Patrikalakis, Cooperative AUV Navigation using a Single Maneuvering Surface Craft, INTERNATIONAL JOURNAL OF ROBOTICS RESEARCH, 29(12)(2010), 1461-1474
[7]. Michael E. West, Vassilis L. Syrmos. Navigation of an Autonomous Underwater Vehicle(AUV) Using Robust SLAM, in: Proc. CACSD, 2006, 1801-1806
[8]. D. Ribas. Underwater SLAM for Structured Environments Using an Imaging Sonar, PhD thesis, Girona University, 2008
[9]. S. Barkby, S. Williams, O. Pizarro, An Efficient Approach to Bathymetric SLAM, in: Proc. IROS, 2009, 219-224
[10]. A. Hwang, W. Seong, Simultaneous Mapping and Localisation for Small Military Unmanned Underwater Vehicle, DEFENCE SCIENCE JOURNAL, 62(4)(2012), 223-227
[11]. A. Hwang, W. Seong, P.M. Lee, Experiment on Simultaneous Localization and Mapping Based on Un -scented Kalman Filter for Unmanned Underwater Vehicles INTERNATIONAL JOURNAL OF OFFSHORE AND POLAR ENGINEERING, 22(1)(2012), 63-68
[12]. I Mahon, S.B. Williams, O. Pizarro and M. Johnson-Roberson, Efficient View-Based SLAM Using Visual Loop Closures, IEEE TRANSACTIONS ON ROBOTICS, 24(5)(2008), 1002-1014
[13]. B. He, H.J. Zhang , C. Li , S.J. Zhang, Autonomous Navigation for Autonomous Underwater Vehicles Based on Information Filters and Active Sensing, SENSORS, 11(11)(2011), 10958-10980
[14]. B. He, Y. Liang, X. Feng , R. Nian, AUV SLAM and Experiments Using a Mechanical Scanning Forward -Looking Sonar, SENSORS, 12(7)(2012), 9386-9410
[15]. Gillijins S, Barrero M, Chandrasekar B, et al. What is the ensemble Kalman filter and how well does it work [C] II Proc. of the American Control Conference, 2006: 4448-4453.